Domain-specific functionalization of cellulose fibers via itaconic anhydride-mediated esterification

Cellulose (2026) 33:3143–3159
https://doi.org/10.1007/s10570-026-07011-5

ORIGINAL RESEARCH

Domain-specific functionalization of cellulose fibers via itaconic anhydride-mediated esterification

Jelka Feldhusen · Per Tomas Larsson · Kent Malmgren · Gunnar Westman

Received: 31 July 2025 / Accepted: 11 March 2026 / Published online: 24 March 2026

Abstract Softwood kraft pulp is known to produce one of the strongest papers, with main application areas in tissues, packaging, and high-quality or specialty papers. These tailored applications often crave chemical modification of the fibers to optimize and tailor their inherent properties. This paper presents two scalable methodologies, gas phase reactions and kneading reactions, for the esterification of bleached kraft pulp (BKP) with itaconic anhydride (ITA). Itaconic anhydride is bioderived with a structure similar to succinic or maleic anhydride, two commonly used chemicals for modifying pulps to introduce charge groups on the cellulose fibers. Although similar in structure, itaconic derivatives also contain an exocyclic, out-of-chain unsaturation, which is useful for additional chemical modifications, such as Michael additions and polymerization reactions. The modification of BKP was performed on never-dried and water-free pulp, aiming to produce highly charged fibers while preserving the overall fiber structure and thereby their intrinsic properties. The reaction yields were investigated by varying molar ratio, temperature, and reaction time, and the modified fibers were characterized using ATR-FTIR, solid state CP/MAS ^{13}C-NMR, XRD, titration techniques, and water retention values. The different modification methods showed differences in the spatial distribution of the substituents, preferably modifying the fiber surface or the fiber wall interior. In general terms, modifications facilitated through kneading showed a higher degree of modification of the fiber wall interior, whilst gas-phase mediated reactions preferentially modified the fiber surface. This allows for tailoring the location of the modification, decorating the fibers within or on the surface, and opening routes for a customizable pulp.

Supplementary Information The online version contains supplementary material available at https://doi.org/10.1007/s10570-026-07011-5.

J. Feldhusen · G. Westman (✉)
Department of Chemistry and Chemical Engineering, Chalmers University of Technology, Kemivägen 10, 41296 Gothenburg, Sweden
e-mail: westman@chalmers.se

J. Feldhusen · G. Westman
Wallenberg Wood Science Center, Chalmers University of Technology, Kemivägen 10, 41296 Gothenburg, Sweden

P. T. Larsson
Department of Fiber and Polymer Technology, School of Chemical Science and Engineering, KTH Royal Institute of Technology, Teknikringen 56, 10044 Stockholm, Sweden

P. T. Larsson
Wallenberg Wood Science Center, KTH Royal Institute of Technology, Teknikringen 56, 10044 Stockholm, Sweden

K. Malmgren
SCA, Senior R&D Specialist, Sundsvall, Sweden

Keywords Itaconic anhydride · Gas-phase modification · Kneading reaction · Fiber charge · Bleached kraft pulp (BKP) · Wet-strength properties

Introduction

It is well known that paper loses strength and structural integrity when exposed to water. A common strategy to mitigate this loss is to incorporate wet-strength functionality, either through chemical modification of the pulp, hydrophobization, or sizing, or by the addition of wet-strength agents. Depending on the type of wet strength or hydrophobization agent, the addition is performed at different stages along the paper production line. Most of the commonly used wet strength agents are added to the pulp during the manufacturing process before the sheet is formed, that is, at the "wet end" of the process. However, additives that are not rapidly absorbed by pulp fibers must be added after sheet formation, to form a micro-thin layer on the paper surface (Francolini et al. 2023) or pressing the reagents into the sheet.

By introducing itaconic acid (H_2IA) on or within the fibers, effectively decorating them with both a carboxylic acid and an unsaturation, a multi-functional pulp is created which, either by itself, may bind water through its carboxyl groups or further be modified and tailored for desired properties. Common wet-strength agents either form covalent bonds between the fibers, thereby creating cross-links (Roberts 1996; Ek et al. 2009, Tom Lindström 2005/2018) or impart pH-sensitive groups (Tarrés et al. 2018; Onur et al. 2019) as in carboxylic functionalized fibers. One of the most dominant cellulose-based wet-strength agents is poly(aminoamide)-epichlorohydrin (PAE), often used in combination with carboxymethylcellulose, CMC (Espy 1995; Onur et al. 2019). Although effective, the use of PAE and similar compounds has raised concerns due to the risk of emission of adsorbable organic halides (AOX) into wastewater streams, creating a desire to limit their use, and a pull to find and develop new cross-linkers with less environmental concerns.

Maleic and succinic anhydride are also widely utilized as they decorate the fibers with carboxylic acid functionalities, and are often used in combinations with other compounds to introduce desired properties. The sizing agent alkenyl succinic anhydride (ASA), is synthesized from maleic anhydride and unsaturated petrol-based compounds, acting as a hydrophobization agent due to their long carbon chain. From previous studies on anhydride functionalization of cellulose, Zhang et al. explored the possibility of using maleic anhydride polymer for the carboxylation of bleached kraft pulp, gaining fibers with surface charges ranging from 0.05–0.13 meq/g (milli-equivalents of charge per gram pulp) depending on the polymer created from the anhydride used (Zhang et al. 2021). Similarly, direct grafting of succinic and maleic anhydride on microfibrillated cellulose has been reported by Stenstad (Stenstad et al. 2008), gaining DS values of 0.8 and 0.3 for the succinic and maleic acid, respectively, corresponding to approximately 1–3 meq/g. TEMPO-oxidization of fibers, which also introduces a carboxylic acid functionalities to the fiber, was initially evaluated as wet-strength agent and gave significantly enhanced wet-strength; however, the use of TEMPO as wet-strength agent has been overshadowed by the great interest of TEMPO-oxidized pulp defibrillated to stable cellulose nanofibril (CNF) suspensions. (Isogai et al. 2011) and has now been scaled to industrial production by Nippon Paper (Industries, 2025).

In comparison to maleic or succinic anhydride, itaconic anhydride (ITA) introduces an exocyclic, out-of-chain unsaturation making it unsymmetrical, creating two structurally different esters, expanding alternatives for selective crosslinking or hydrophobization (Fig. 1).

In this study, we investigate the derivatization of bleached kraft pulp (BKP) with itaconic anhydride and its use as a potential wet-strength additive/enhancer, whilst preserving the inherent benefits of cellulose-based systems. Key motivations for exploring itaconic anhydride (ITA) derivatization lies both in its unique chemical structure and properties, enabling a variety of modifications and multi-step derivatizations, and that itaconic acid has been envisaged to become one of the future major bio-feedstock chemicals. Itaconic acid (H_2IA), the precursor of ITA, is bio-based and is produced synthetically from citric acid or through the fermentation of sugars in microorganisms. The multifunctional monomer with a polarized α, β-unsaturation provides a distinct functional handle for further chemical modifications by different conjugate additions.

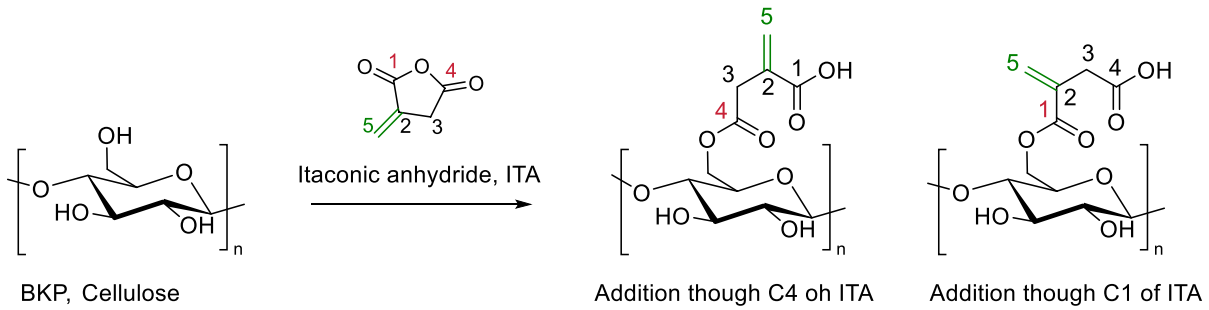

Fig. 1 Chemical modification of bleached kraft pulp (BKP) with itaconic anhydride (ITA), through the ring-opening at the C1 or C4 carbon in ITA. Left: Structure of cellobiose. Right: Esterification through C4, respectively C1 of itaconic anhydride (ITA)

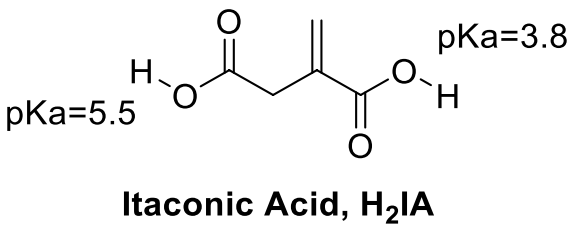

Fig. 2 Chemical structure of itaconic acid, H_2IA, with two distinct pK_a values of the respective carboxylic acid

The two carboxylic acids in H_2IA have different pKa values, as seen in Fig. 2. Depending on which of the carbonyl groups form an ester with the pulp (see Fig. 1), the remaining carboxylic acid function may be used for further modification. However, it must be considered that the conjugated H_2IA to fibers may express shifted pK_a values compared to H_2IA, due to intramolecular hydrogen bonds from cellulose to the carbonyl groups on the itaconate. (Shokri et al. 2012).

Further, the carboxyl group present in ITA esterified BKP, from here on BKP-itaconate, extends a few atoms further away from the cellulose surface, as compared to for example carboxylic groups in TEMPO-modified fibers and CMC. This spatial arrangement most probably results in differences in interactions with the interfacial water layers surrounding the cellulose, potentially affecting hydration dynamics and adhesion properties. These features may give itaconic acid-modified fibers properties that complement or surpass existing cellulose-based wet-strength agents, and be used for those applications in future studies.

The objective of this study is to explore two methods of derivatization, either by kneading of never-dried BKP (BKP_{ND}) or liquid-exchanged BKP (BKP_{LE}) with ITA, or through gas-phase reaction with BKP_{LE}. The main way of evaluating the effectiveness of the modification was by normalization of the signals for carbonyl groups with the C–O–C signal at 1160 cm^{-1} in cellulose using FTIR. After refining the conjugation process, the itaconic acid-modified cellulose material was evaluated for its wet-strength performance, surface characteristics, and interaction with water, providing key insights into its potential as a cellulose-based wet-strength additive. The aim of this study is therefore to evaluate the esterification of bleached kraft pulp with itaconic anhydride using two scalable methodologies, kneading and gas-phase reactions, and to assess how these routes influence the spatial distribution of substitution within the fiber structure. Based on previous reports, kneading is expected to facilitate penetration of the reagent into the fiber wall, whereas gas-phase esterification is anticipated to primarily modify the fiber surface. Furthermore, as itaconic anhydride exhibits a reactivity toward cellulose comparable to that of maleic anhydride but provides an asymmetric structure and a highly reactive exocyclic double bond, it may offer additional possibilities for subsequent polymerization reactions. These combined features make itaconic anhydride an attractive precursor for the preparation of polymer-substituted fibers. In the result section we present the results of these investigations starting from the properties of the obtained BKP-Itaconate before detailing the strategy that led to the reaction conditions used for the final material properties.

Experimental

Materials

All chemicals were purchased and used without further purification. Itaconic anhydride (95%), Sodium hydroxide (97%), and hydrochloric acid (37%) were purchased from Sigma Aldrich, Acetone and Acetonitrile from Fisher Scientific, and ethanol (95%) from Solveco. Deionized water was used in all cases except for titrations where MQ-water (18.2 MΩcm at 25 °C, filtered by a Stathmos Sartorius machine) was used. Never dried softwood bleached kraft pulp (BKP) was kindly provided by Billerud Korsnäs (Sweden) and used as delivered (BKP_{ND}) or liquid exchanged with ethanol and acetonitrile before use (BKP_{LE}). A carbohydrate analysis of BKP_{ND} showed a relative cellulose content of 80%, hemicellulose of 18.4%, and lignin content of 1.6%, BKP_{LE} was found to have 86% cellulose, 12.3% hemicellulose and 1.7% lignin (SI, Table S2). Avicel, MCC from cotton linter, was purchased from Sigma Aldrich and used without further modifications.

Methods

Kneading reaction, BKP_{ND} (BKP_{ND} Kn)

Never dried BKP (13–17 wt.%), BKP_{ND}, was combined with itaconic anhydride by adding pulp and anhydride together in a plastic vial. The mixture was alternately shaken and mixed with a spatula for a total time of approximately 10 min. Larger batches were instead placed in a plastic bag that was kneaded by hand.

The pulp was thereafter placed on a petri dish and set in an oven for varying times at different temperatures, depending on the reaction. After modification, the pulp was washed with acetone and water until the conductivity of the filtrate was below 5 µS. An appropriate amount of HCl 0.1 M (10 mL/0.5 g dry cellulose) was added to secure that all carboxylic acid was in protonated form, followed by a small amount of deionized water to remove excess acid. The pulp was left to dry on a bench at room temperature overnight before further analysis.

Molar ratios were set and calculated by dividing the dry weight of the fiber by the molecular weight of one AGU. A 1:1 ratio of AGU:ITA would correspond to equimolar amount of the reagents, 1:0.1 would correspond to number of moles multiplied by 0.1 for moles of ITA added.

Liquid exchanged BKP, BKP_{LE}

100 g of BKP_{ND} (12–14 wt. %) was washed and filtered with 3×250 mL ethanol, followed by 250 mL acetonitrile. Fibers were oven-dried overnight at 40 °C before further use. For larger batches (above 30 g dry fiber mass), the pulp was allowed to swell covered in ethanol (approximately 1 L) for 30 min before filtering. The filter cake of fibers was washed with an additional 400 mL of ethanol before resuspending again in ethanol for 30 min, filtered, and washed. In the last step, the fibers are suspended and washed in acetonitrile before being allowed to dry on the bench for 30 min before being placed in an oven at 40 °C overnight. The mol equivalences were calculated as described above in.

Kneading reaction, BKP_{LE} (BKP_{LE} Kn)

BKP_{LE} was placed in a plastic vial to which itaconic anhydride dissolved, amounts see Table 1, in a small amount of acetone (approximately 1 mL/0.1 g dry pulp) was added. The reagents were combined as described for BKP_{ND} Kn—reactions, before being poured onto a glass petri dish left on the bench for 15 min for the solvent to evaporate. For larger-scale reactions (10–60 g), the ITA was mixed through massaging in a plastic bag. The pulp was transferred to a glass petri dish and placed in the oven at the desired temperature and time until all solvent was evaporated. The modified pulp was again washed and left to dry, as described above, before further analysis. The mol equivalences were calculated as described above. Control reactions with Avicel were done as presented in the Supplementary Information, Figure S6.

Gas-Phase reaction (BKP_{LE} Gas)

The gas phase reactions were based on a patent by Malmgren et al. (Malmgren and Nordqvist 2023). In

Table 1 Water absorption and charge for fibers through different modification methods, kneading or gas-phase reaction

Reaction	NaOH titration (meq/g)	DS	WRV (g/g)	Tea bag (g/g)	Surface charge (μeq/g)	Total charge (μeq/g)
BKP_{ND}	0.14 ± 0.0065	0.0231	0.98 ± 0.02	30.5 ± 1.5	6	29.4
BKP_{ND} Kn_1_80°C_1 g	0.50 ± 0.03	0.0866	0.70 ± 0.05	36.0 ± 2.2	n.d	n.d
BKP_{ND} Kn_0.5_80°C_0.5 g	0.35 ± 0.04	0.0594	0.84 ± 0.02	42.3 ± 1.7	n.d	n.d
BKP_{ND} Kn_0.5_80°C_12 g	0.32 ± 0.04	0.0541	0.84 ± 0.02	42.3 ± 1.7	11.5	108.3
BKP_{LE}	0.085 ± 0.02	0.0139	1.09 ± 0.06	42.4 ± 2.2	12.4	34.8
BKP_{LE} Kn_1_70°C_0,5 g	0.65 ± 0.02	0.1149	0.89 ± 0.09	46.0 ± 7.4	n.d	n.d
BKP_{LE} Kn_0.2_70°C_12 g	0.50 ± 0.01	0.0866	0.75 ± 0.1	32.5 ± 2.3	n.d	n.d
BKP_{LE} Kn_0.1_70°C_60 g	0.35 ± 0.01	0.0594	0.81 ± 0.2	28.1 ± 5.8	18.6	128.4
BKP_{LE} Kn_0.035_70°C_1 g	0.26 ± 0.015	0.0436	0.83 ± 0.05	37.3 ± 5.9	n.d	n.d
BKP_{LE} Gas_1_75°C_2 g	0.38 ± 0.03	0.0647	0.68 ± 0.02	40.5 ± 3.1	n.d	n.d
BKP_{LE} Gas_1_75°C_10 g	0.28 ± 0.03	0.0471	0.68 ± 0.02	40.5 ± 3.1	43.9	128.4
BKP_{LE} Gas_0.1_75°C_2 g	0.50 ± 0.03	0.0866	0.77 ± 0.03	35.4 ± 2.1	n.d	n.d
BKP_{LE} Gas_0.01_75°C_2 g	0.18 ± 0.02	0.0299	0.82 ± 0.05	34.5 ± 2.2	n.d	n.d
BKP_{LE} Gas_1_50°C_2 g	0.28 ± 0.05	0.0471	0.85 ± 0.07	32.4 ± 3.1	n.d	n.d

a glass petri dish at the bottom of a desiccator, a predetermined amount of itaconic anhydride was placed. A metal mesh grid was placed above the anhydride with BKP_{LE} placed on it without direct contact with the anhydride. The BKP_{LE} was lightly fibrillated using a kitchen mixer for 3 × 10s before placement onto the metal mesh in the desiccator. The lid was closed, and the desiccator containing ITA and BKP_{LE} was placed into the oven at the required temperature and time, see Table 1. The volume of the desiccator used is 2,8 dm^3. After the reaction, the fibers were allowed to cool and were then washed and stored as for the other reactions.

FTIR

The ATR-FTIR spectra were collected on a Vertex70v FTIR spectrometer, 4000–400 cm^{-1}, 32 scans with a resolution of 4 cm^{-1}. The background was collected before the recording of the spectra. For each spectrum, background subtraction and baseline correction were performed using the adjacent software, and the data was normalized to the cellulose glycosidic bond (C–O–C) antisymmetric stretching vibration at 1160 cm^{-1} (Salmén and Stevanic 2018).

Carboxylic acid content and degree of substitution (DS)

Titrations were performed using a Metrohm 888 Titrando titration apparatus with 0.01 M NaOH. For each sample, approximately 200 mg of fibers were dispersed in 30 mL MQ-water and stirred overnight. Before titration, 40 µl 0.5M NaCl was added and the pH of the suspension was adjusted to 2.7–3.2 with 1 M HCl, to protonate the itaconic aid functionalities. The charge was calculated based on the last determined equivalence point for the titration and corrected for the addition of HCl according to Eq. 1:

$$Carboxylic\ acid\left[\frac{mmol}{g}\right] = \frac{c * (V2 - V1)}{m} \quad (1)$$

where V1 is the volume of NaOH (mL) needed to neutralize the known amount of HCl added, V2 is the volume of NaOH (mL) at the last equivalence point, c is the concentration of NaOH (M), and m is the mass of fibers titrated (g). (Beatson 1992; Lindgren et al. 2002; Åhl et al. 2025).

The degree of substitution was assessed through the carboxylic acid content according to Eq. 2, based on the work of Wongvitvichot et al. (2021).

$$DS = \frac{AGU * C}{1000 - (SG * C)} \quad (2)$$

where AGU = 162 g/mol, C is the carboxylic acid content (mmol/g) as determined through titration and SG is the substituting group, here itaconic acid of 129 g/mol, calculated as the molecular weight of 130 g/mol with one hydrogen subtracted due to the esterification.

The reaction efficiency was calculated as a ratio between final fiber charge and amount of ITA used for the reaction, calculated in mol/g in both cases and multiplied by 100, gaining a relative percentage of reaction efficiency. The data is found in the Supplementary Information, Table S1.

Measurement of surface and total charge

Polyelectrolyte titrations were performed based on a method developed by Winter et.al (Winter et al. 1986), using poly(diallyldimethylammonium) chloride (polyDADMAC, Alcofix 132 from Allied Colloids, cut off 300,000 Da) and PolyBRENE (Sigma Aldrich, molecular weight of 4,000–6,000 g/mol). For each type of fiber, the fibers were washed in 10 mM $NaHCO_3$ for 1h before rinsing with deionized water to neutral pH. For each point, 1 g (dry) of fiber was added to an E-flask. To this, the desired amount of polymer (poyDADMAC or polyBRENE) was added and filled with MQ-water to a total mass of 100 g. The sample was stirred for 30 min, after which the suspension was filtered, the filtrate saved, and the fibers dried. 10 g of the filtrate was titrated with potassium polyvinyl sulfate (KPVS, Wako Pure Chemical Industries) using a particle charge detector (PCD 03 equipment from BTG Mütek). The sorption isotherm curve was produced by plotting samples with different polymer loading, gaining the surface or total charge of the fibers through the charge density of the adsorbed polymer. For each curve, a minimum of 5 samples were tested with different loadings of polymer (see SI, Figure S7 for details).

CP/MAS ^{13}C-NMR CP/MAS ^{13}C-NMR spectra were recorded on pulp fibers. Fibers were packed at ambient conditions in zirconium rotors and ran at 298 K on a Bruker Avance III 500 MHz spectrometer, equipped with a 4mm HX CP/MAS probe. A contact time of 1.5 ms and a repetition time of 2s were recorded at a magic angle spinning rate of 10 kHz. 4000 scans were collected for each sample. The dataset was normalized to have the same intensity at the 89 ppm signal to explore the C4 region of the spectra. The relative intensity of the C4 region (80–92 ppm) was compared to the normalized 89 ppm signal for assessing the relative degree of modification. The unit-less relative surface signal intensity, that is the stochiometric surface-to-volume ratio q was calculated and is presented in the Supplementary Information, Table S3, alongside the standard error.

Tea-bag test and water retention value (WRV)

To estimate the water binding capacity, g water/ g cellulose, of the samples, Tea bag test and water retention values were measured in triplicate as described by Börjesson *et. al.*, slightly adapted for this study. (Borjesson, Richardson et al. 2015) For the tea-bag tests, fibers were swelled in 20 mL of water for 4h, before allowing them to drip through the centrifuge filter overnight. Once dripping had ceased, the fibers were weighed ($m_{wet\ fibers\ after\ dripping}$), spun, and dried at 105 °C ($m_{dried\ fibers}$) to assess their water-holding capacity. The tea-bag value was calculated as in Eq. 3.

$$Tea - bagvalue = \frac{m_{wetfibresafterdripping}}{m_{driedfibres}} \quad (3)$$

100 mg of pulp was suspended in deionized water for 4h, after which the fibers were placed on a filter (pores 45 µm) within a centrifuge tube and allowed to drip freely overnight. Thereafter, the self-dripped water was discarded, and the fibers were spun through centrifugation for 15 min at 3000G. The fibers were weighed, gaining $m_{wet\ fibers}$, before placement in the oven for drying at 105 °C for 24h, $m_{dry\ fibers}$. The WRV was calculated based on the wet and dry mass of the pulp as in Eq. 4.

$$WRV = \frac{m_{wetfibres} - m_{driedfibres}}{m_{driedfibres}} \equiv \frac{m_{water}}{m_{driedfibres}} \quad (4)$$

X-ray diffraction, XRD

Reflection mode XRD was used to estimate the crystallinity of different pulps/materials before and after chemical modification. The sample was placed on a zero-background sample holder (single silica-crystal) and data was collected between $5° \leq 2\theta \leq 55°$, with a step size of 0.020° on a D8 Discover (Bruker) XRD, with Cu-Kα radiation of 1.5418 Å ($\lambda_1 = 1.54060$ and $\lambda_2 = 1.54439$ Å, estimated as 1.5418 Å). The samples were baseline-corrected by subtracting a blank sample from the collected data, correcting for background scattering. The data was smoothed using adjacent averaging, a 5-point window. For the evaluation, the signal from the reflection plane (200) was fitted with a Gaussian function, using the interval 17–27° and the Scheerer equation was used for the measurement of average crystallite size, L as in Eq. 5,

$$L = \frac{0.9\lambda}{\beta cos\theta} \tag{5}$$

where λ is the incident X-ray wavelength, 0.9 is the shape factor, β is the full width at half maximum (FWHM) of the Gaussian fitted to the (200) reflection in radians, and θ is the position of the signal maximum of the (200) reflection. (Scheerer 1918; Patterson 1939; French and Santiago Cintrón 2013). The instrumental broadening was subtracted from the FWHM before use in the Scherrer equation. For assessing the relative degree of crystallinity, Segal's method was used, displayed in Eq. 6, comparing the intensity of the (200) reflections as I_{200}, with the intensity corresponding to the amorphous contribution, I_{am}, of the sample found between 18–19°.

$$CrI = \frac{I_{200} - I_{am}}{I_{200}} \times 100 \tag{6}$$

Results

With the attempt to optimize the reaction efficiency a screening study by varying reaction time, temperature, and AGU:ITA molar ratio/equivalences, was conducted. For kneading reactions of never dried fibers, an optimal ratio of 1:0.5 (AGU:ITA) at 80 °C was found, and for the liquid exchanged fibers, a reaction time of 30 min at 70 °C, and a molar ratio of 1:1 gave the highest carbonyl content. For the gas phase reactions, a molar ratio of 1:1 (AGU:ITA) at 75 °C gained the strongest carbonyl signal. See Table 1 for more details and presentation of how reaction conditions affect reaction efficiency. It should be noted that certain limitations are implanted in this study, as for example a maximum ratio if AGU:ITA was set as 1:1.

Water retention and fiber swelling and their correlation to fiber charges

The Tea-bag test measures the water between fibers and inside the fiber lumen, whereas WRV mainly quantifies the water retained within the fiber wall (Jayme 1958; Abson and Gilbert 1980; Weise et al. 1996). Fiber wall charge, chemical composition, pore volume, specific surface area, and drying history are all fiber wall properties that can influence WRV. Although WRV measurements do not provide absolute values that can be directly compared across different fiber sources, since water removal during centrifugation depends on species and fiber morphology, they are useful for identifying trends within the same study. Correlating the water sorption profile and the total/surface charge (Table 1) reveals slight trends among the different treatment processes. The liquid-exchanged pulp, BKP_{LE}, had a relatively low total charge of 34.8 µeq/g and a surface charge value of 12.4 µeq/g with the highest WRV value. Interestingly, the never-dried BKP, BKP_{ND}, expressed a similar WRV value but with significantly lower surface charge, 6µeq/g, and a total charge of 29.4 µeq/g, similar to BKP_{LE}, having a total charge of 34.8 µeq/g.

Between these samples, a significant change in tea-bag value was also observed. This together would indicate that although the ability to hold fiber wall water is similar (similar WRV values), the process of exchanging the liquid in BKP_{LE} influences both the charge distribution and ability to retain inter-fiber water, most likely due to slight structural changes, i.e. removal of hemicellulose and thereby change in interactions, as also seen in the carbohydrate analysis (SI, Table S2). Accessibility is also thought to be the reason for the non-linear relation between total surface charge and degree of substitution, as seen for example for BKP_{ND} and BKP_{LE}, much likely due to the removal of hemicellulose and rearrangement of the supermolecular structure.

The numbers in the labelling of compounds, BKP_{LE} Kn_1_70°C_0,5g, are as follows _1_ is the mol equivalence AGU:ITA, _70°C_, is the reaction temperature, and 0,5g is the dry weight of fiber in the experiment. Large-scale reactions were planned based on FTIR studies and chemical use.

The larger-scale reaction of 60 g of kneaded liquid-exchanged modified pulp, BKP_{LE} Kn_0,1_70°C_60 g, exhibited the lowest Tea-bag water absorption (28 g/g) among the samples, while its WRV (0.81 g/g) was lower than that of the unmodified fibers. The total charge (128.4 µeq/g) and surface charge (18 µeq/g) were significantly higher than that of unmodified fibers of BKP_{LE} (34.8 µeq/g and 12.4 µeq/g, respectively). The reduced WRV suggests that liquid exchange introduces additional structural changes that limit fiber swelling and accessibility for liquids to the interior parts of the fiber wall. This might be due to an increased wet strength from the itaconic ester and/or hornification occurring during drying. The slightly lower WRV compared to unmodified fibers indicates that some capacity for fiber wall water retention is lost. The high total charge in combination with the relatively low surface charge implies that these modifications primarily occur in the interior parts of the fiber wall rather than on the fiber surface, reducing fiber wall swelling and leading to a lower overall water absorption.

In contrast, the gas-phase modified pulp, BKP_{LE} Gas_1_75°C_10 g, exhibited a tea-bag water absorption value of 40.5 g/g, similar to the unmodified fibers, but a significantly lower WRV of 0.7 g/g. The total charge increased substantially to 128.4 µeq/g for BKP_{LE} Kn_0.1_70°C_60 g, while the surface charge here rose to 43.9 µeq/g.

Finally, for the kneading reaction of never dried fibers, BKP_{ND} Kn_0.5_80°C_12 g gave a surface charge of 11.5 µeq/g and a total charge of 108.3 µeq/g. The low surface charge may be due to that ITA hydrolysis into the less reactive itaconic acid (H_2IA) in water, before moving deeper into the fiber wall. During drying, after enough time when the water content is low, the unreacted acid converts into the anhydride, which then reacts with the fibers. Speculatively, it may be that the method of liquid exchange results in the fibers exposing more reactive hydroxy groups on fiber surfaces, and that fibrils restructure and reform during drying, which may regain losses in WRV values. This would mean that the WRV value is a product of the integration of charges (classically increasing WRV), whilst structural changes in the fibers act to lower the WRV.

Generally, for reactions performed by kneading, the surface charge is lower than compared to the gas-phase reaction, given that for the kneading reaction, the reagents are forced by mechanical kneading and by so, govern the reagents to penetrate deeper into the fiber wall. However, it should also be stressed that the assessment of surface and total charges using polyDADMAC and polyBRENE, only measures accessible groups, which may be limited due to confinement issues and electrostatic interactions.

Having established how properties correlate to reaction conditions, it is essential to understand the underlying process that led to these results. It should also be noted that although reactions are performed in the same manner and in several repetitions, changes are observed within the same series due to the heterogeneity in fibers and the kneading process. To get further information on the details of itaconic grafting to BKP, CP/MAS ^{13}C-NMR and FTIR analysis were used.

CP/MAS ^{13}C-NMR and XRD

Solid-state CP/MAS ^{13}C-NMR spectra were recorded directly on the modified pulp fibers to investigate structural changes induced by esterification. The carbonyl resonance of the itaconate functionality would ideally appear between 160–180 pm, however, at low degrees of substitution (DS < 0.02) these signals are often undetectable due to the weak cross-polarization of unprotonated carbons (David et al. 2019).

Figure 3 shows representative spectra for kneaded BKP_{ND} and BKP_{LE} samples, as well as gas-phase modified BKP_{LE}. As previously described by Hult et al. (2002), the C4 region (80–92 ppm) is particularly diagnostic: resonances at 89.5, 88.8, and 87.9 ppm correspond to crystalline cellulose Iα, I(α + β), and Iβ, respectively, while signals at 88.7, 84.3, 83.8, and 83.3 ppm originate from

Fig. 3 CP/MAS ^{13}C NMR. Top: BKP_{ND} Kn-reactions, Middle: BKP_{LE} Kn-reactions, and Bottom: BKP_{LE} Gas-reactions. The left panel shows the complete collected spectra of each sample, the right a close-up on the region between 92–80 ppm, showing the changes in the C4 region normalized to the signal of 89 ppm

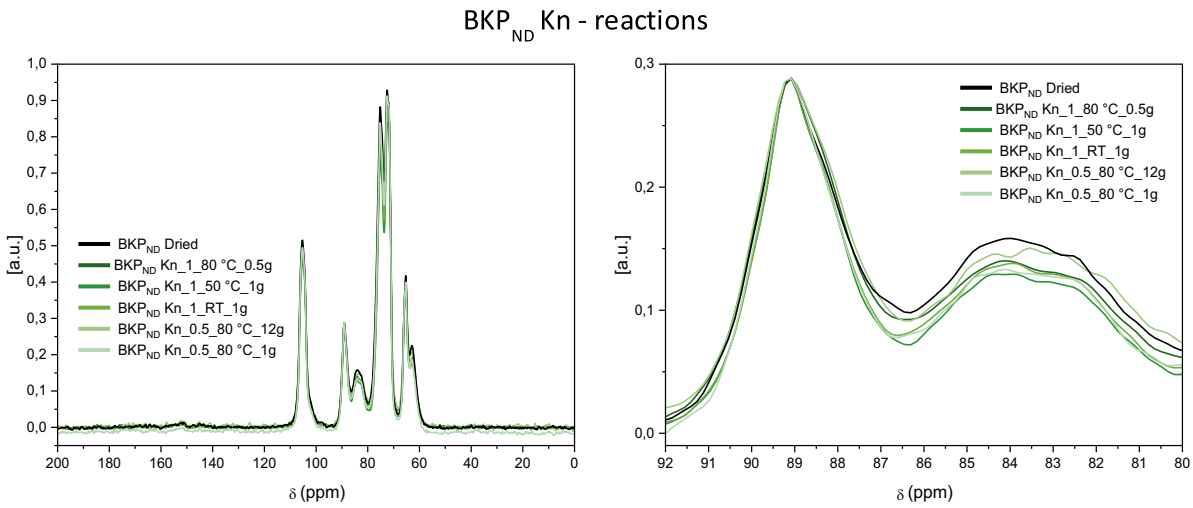
BKP$_{ND}$ Kn - reactions
[a.u.]
δ (ppm)
BKP$_{ND}$ Dried
BKP$_{ND}$ Kn_1_80 °C_0.5g
BKP$_{ND}$ Kn_1_50 °C_1g
BKP$_{ND}$ Kn_1_RT_1g
BKP$_{ND}$ Kn_0.5_80 °C_12g
BKP$_{ND}$ Kn_0.5_80 °C_1g

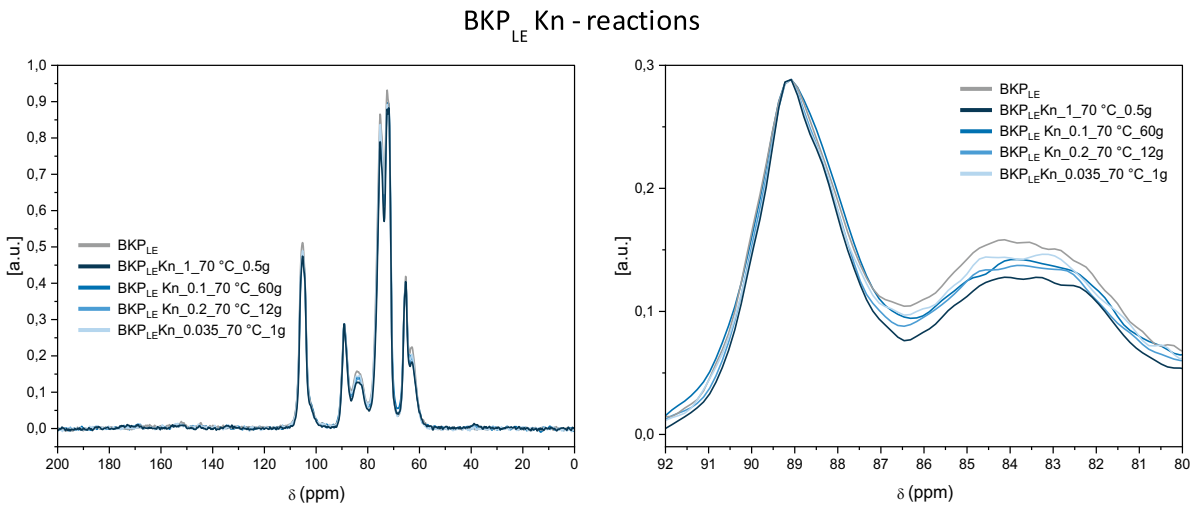
BKP$_{LE}$ Kn - reactions
[a.u.]
δ (ppm)
BKP$_{LE}$
BKP$_{LE}$Kn_1_70 °C_0.5g
BKP$_{LE}$ Kn_0.1_70 °C_60g
BKP$_{LE}$ Kn_0.2_70 °C_12g
BKP$_{LE}$Kn_0.035_70 °C_1g

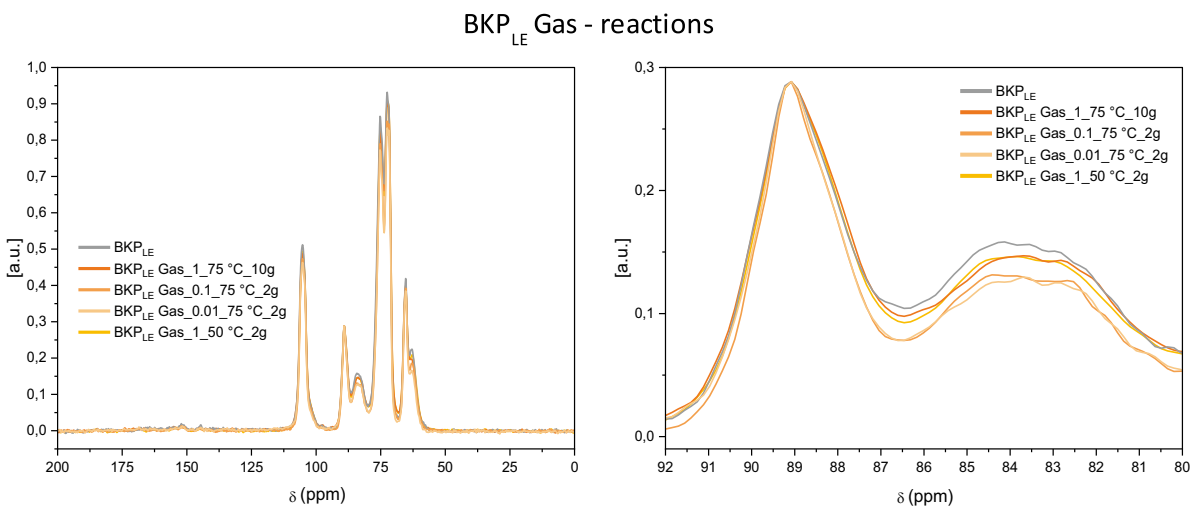
BKP$_{LE}$ Gas - reactions
[a.u.]
δ (ppm)
BKP$_{LE}$
BKP$_{LE}$ Gas_1_75 °C_10g
BKP$_{LE}$ Gas_0.1_75 °C_2g
BKP$_{LE}$ Gas_0.01_75 °C_2g
BKP$_{LE}$ Gas_1_50 °C_2g

para-crystalline domains and accessible or inaccessible fibril surfaces. Minor contributions from hemicelluloses can also appear near 81–82 ppm (Wickholm et al. 1998; Terrett et al. 2019). Modification of surface polysaccharides typically causes broadening and/or intensity loss of the C4 surface peaks around 83–84 ppm relative to the crystalline signal at 89 ppm. The decreasing intensity of these surface-related resonances with increasing charge density (Table 1) therefore confirms chemical substitution at fibril surfaces. Both BKP_{ND} Kn and BKP_{LE} Kn reactions follow this trend, showing reduced C4 surface intensity for samples with higher carboxyl content (e.g. 0.65 meq g^{-1} vs. 0.26 meq g^{-1}). These spectral changes confirm successful esterification and demonstrate that even subtle modifications of the fiber wall can be captured by careful solid-state NMR analysis. The relative surface to volume ratio of the collected signal can be found in Supplementary Information, Table S3.

X-ray diffraction (XRD) was used to evaluate changes in the crystallite size of the cellulose fibers after esterification. Representative diffraction patterns for kneaded and gas-phase reactions are shown in Fig. 4, and the corresponding crystallite sizes (French

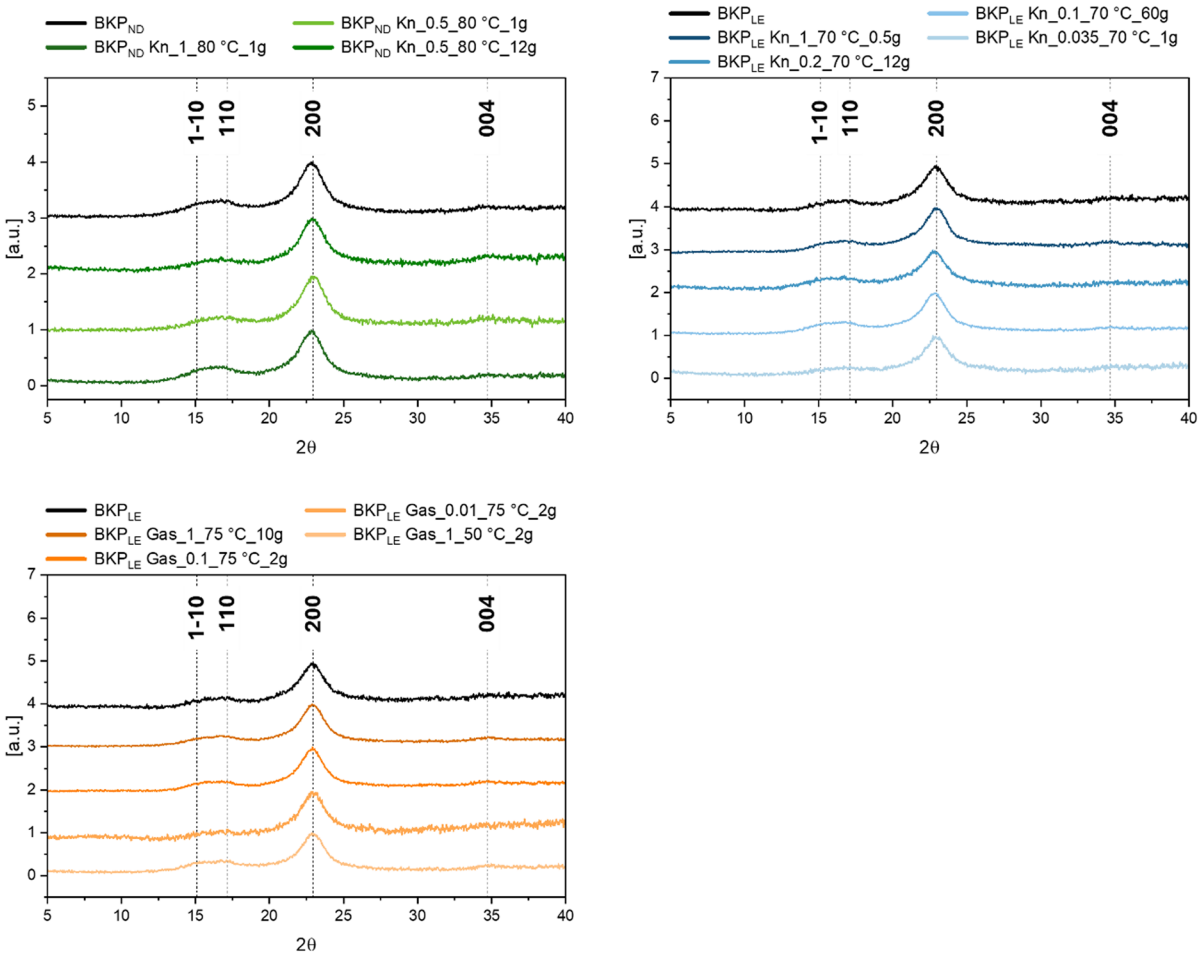

Fig. 4 XRD spectra for the different reactions, stacked. Top Left: BKP_{ND} Kn-reaction, Top Right: BKP_{LE} Kn-reaction, Bottom Left: BKP_{LE} Gas reactions. The significant signals for cellulose are seen, showing the 200, 110, 1–10 and 004 plane

& Santiago Cintrón, 2013) derived from the (200) reflection are summarized in Table 2.

All samples display the typical cellulose I pattern with strong reflections at 2θ ≈ 22.5–23° ((200) plane). The other peaks for the corresponding crystal planes, (1–10), (110), and (004), are marked. The Scherrer-based crystallite sizes calculated from the (200) reflection (Table 2) indicate only minor differences between modified and unmodified fibers. Slight increases in apparent crystallite size for some samples are most likely due to slightly different washing and drying cycles alongside densification effects rather than true recrystallization. The crystallinity index also varies along with the samples with no apparent pattern, except for a uniform decrease when comparing reference to modified material apart from BKP_{LE} Gas_0.01_75°C_2 g where a slight increase can be seen. However, this may also be due to the analysis of the spectra where some samples were more difficult to assess than others. These results demonstrate that the esterification—whether by kneading or gas-phase reaction—does not significantly disrupt the crystalline cellulose domains. Instead, the modifications appear to occur primarily in the less ordered regions of the fiber wall, consistent with the NMR observations of surface polymer alteration.

Molecular and structural details and investigation using FTIR

ATR-FTIR spectroscopy was used to confirm the successful esterification of cellulose with itaconic anhydride and to identify characteristic carbonyl and alkene vibrations. Ester formation typically gives rise to a new C=O stretching band around 1720–1735 cm^{-1}, while remaining carboxylic acid groups appear slightly lower, near 1700–1710 cm^{-1}. The presence of unsaturated C=C bonds is expected in the 1630–1650 cm^{-1} region. These assignments might allow differentiation between esterified, protonated, and partially isomerized species. The conjugation to cellulose and local hydrogen bonding can slightly shift these frequencies, but the overall spectral pattern provides a reliable indicator of successful grafting.

More detailed discussions on band assignments, potential isomerization of itaconic acid (to citraconic or mesaconic structures), and literature comparisons for similar systems (maleic and TEMPO-oxidized

Table 2 Summary of average crystallite size (L in Eq. 5) based on the Scherrer equation, given for the (200) plane calculated in degrees and radians

Reaction	2θ max (Degree)	FWHM (Radians)	L(nm)	CrI (%)
BKP_{ND}	22.82	0.032	2.35	81
BKP_{ND} Kn_1_80°C_1 g	22.82	0.031	3.18	80
BKP_{ND} Kn_0.5_80°C_1 g	22.92	0.031	3.98	86
BKP_{ND} Kn_0.5_80°C_12 g	22.84	0.031	2.84	83
BKP_{LE}	22.94	0.031	2.56	97
BKP_{LE} Kn_1_70°C_0,5 g	22.82	0.030	2.95	89
BKP_{LE} Kn_0.2_70°C_12 g	22.73	0.030	3.54	79
BKP_{LE} Kn_0.1_70°C_60 g	22.92	0.031	2.35	81
BKP_{LE} Kn_0.035_70°C_1 g	22.72	0.029	3.35	82
BKP_{LE} Gas_1_75°C_2 g	22.90	0.032	2.45	85
BKP_{LE} Gas_0.1_75°C_2 g	22.90	0.031	3.03	92
BKP_{LE} Gas_0.01_75°C_2 g	22.92	0.029	2.80	97
BKP_{LE} Gas_1_50°C_2 g	22.84	0.030	3.68	79

The instrumental broadening was subtracted from the measured signal. The values of 2θ max are given as maximum of the Gaussian fit between 17–27° of the (200) reflections in degrees. FWHM is the full width at half maximum of the Gaussian fitted to the (200), given in radians. The crystallinity index was calculated with Segal's equation (Eq. 6) using the intensities at the 200 and amorphous region respectively

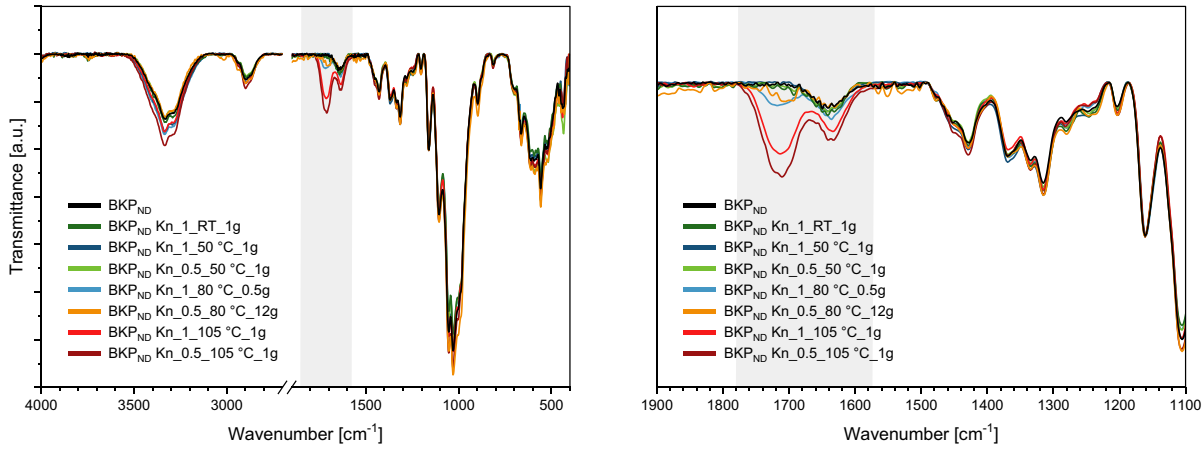

Fig. 5 FTIR spectra of BKP_{ND} Kneading reactions with the grey area highlighting the region of interest. Left: Complete spectra of transmittance versus wavenumber [cm^{-1}]. Right: Closeup of the carbonyl region. In the figure, molar ratios are expressed as AGU:ITA, with BKP_{ND} Kn_1_80°C_1 g being conducted at 80 °C with a 1:1 molar ratio, using 1 g of dry fibers. The relative signal intensity as compared to 1160 cm^{-1} indicates the degree of modification, with a stronger signal indicating more esterification due to the introduction of ester signals in the material. Here, BKP_{ND} Kn_0.5_105°C_1 g shows the strongest signal, indicating the highest degree of modification

celluloses) are provided in the Supplementary Information.

FTIR assessment of the different reactions

FTIR was used as the primary characterization method and used to tune the reaction conditions based on the intensity of the carbonyl signal for BKP_{ND} as presented in Fig. 5. The full spectra for all reactions are found in supplementary information (SI, Figure S3-5). For the BKP_{ND} Kn-reactions, temperatures were varied between room temperature, 50 °C, 80 °C, and 105 °C. Reactions performed at 80 °C and 105 °C show similar trends, with signals present at 1710 cm^{-1} and 1725 cm^{-1} (Fig. 5), most likely coming from the α,β-unsaturated ester or carboxylic acid. Fibers from reaction BKP_{ND} Kn_0.5_105°C_1 g expressed the highest carbonyl-intensity in relation to the normalized peak (C–O–C, 1160 cm^{-1}), also showing the largest intensity around 1640 cm^{-1}, corresponding to water or the C=C bond from itaconic acid.

BKP_{ND} Kn_0.5_105°C_1 g also appears to have several signals overlapping in the 1640 cm^{-1} region, as small shoulders are present around 1631 cm^{-1} and 1650 cm^{-1}, likely due to isomerization of itaconic acid into mesaconic acid, trans-form, or citraconic acid, cis-form. As presented in Fig. 5, the intensity of the carbonyl seems to increase with increasing temperature and molar ratio. However, when reactions were conducted at 105 °C the fibers were difficult to resuspend in water even after stirring in water overnight. We assume this to be due to hornification or cross-linking, and the fibers treated at 105 °C were therefore not investigated further. The carbonyl signal intensity for the two reactions with 1 and 0.5 mol equiv. of reagent conducted at 80 °C expresses similar intensities to one another, whilst no significant increase in the carbonyl signal intensities for reactions at 50 °C and RT were detected compared to the reference material. The similar intensities of BKP_{ND} Kn_1_80°C_1 g and BKP_{ND} Kn_0.5_80°C_12 g most likely occur due to the system being saturated already at a molar ratio of 1:0.5 or that kneading is not as effective in the 12 g reaction. Reaction on a 1 g scale, BKP_{ND} Kn_0.5_80°C_1 g, also presented this behavior, indicating that the first explanation of reaching a saturation point/equilibrium at 1:0.5 seems more likely.

For BKP_{LE} Kn-reactions, two reaction series were performed. One to assess the drying time in the oven, varied between 0 and 120 min at 70 °C, and one at the optimal drying time for that batch size with varying AGU:ITA ratios. For the drying time, it was established that 30 min at 70 °C resulted in the largest carbonyl signal (SI, Figure S3), whilst it was also

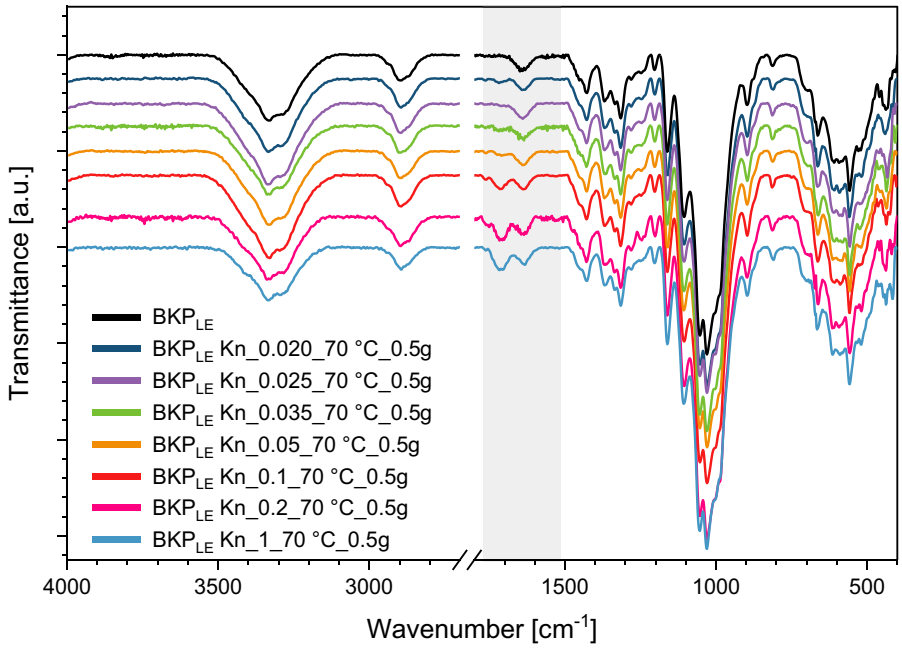

Fig. 6 FTIR spectra of BKP_{LE} Kneading reactions at 70 °C with different mol equivalences of AGU:ITA. Equivalences between 1:1 and 1:0.020 were explored, where an increase in the relative carbonyl intensity compared to the 1160 cm^{-1} signal of cellulose can be observed, indicating an increase in modification

realized that the reaction occurred instantly at room temperature, but less efficiently. For the different molar ratios, 1, 0.2, 0.1, 0.05, 0.035, 0.025, 0.02, carbonyl signals were present but became weak at ratios below 0.035, as seen in Fig. 6.

In the spectra of the modified fibers three distinct signals are seen at 1704 cm^{-1}/1717 cm^{-1} (C=O) and a weak/hardly seen signal at 1762 cm^{-1}. The C=C appears around 1632 cm^{-1}, with another signal at 1660 cm^{-1}, and with a shoulder sometimes occurring around 1691 cm^{-1}, once again indicating isomerization of itaconic acid into citraconic or mesaconic acid. For the reaction performed in a water-free environment, with a small amount of acetone as solvent for the anhydride to facilitate mixing, it seems that reaction conditions promote the anhydride to react differently compared to reactions with BKP_{ND}, i.e., preferring to ring-open at the C1, rather than C4 in ITA, or isomerizing into other species. The control reaction conducted with microcrystalline cellulose (MCC) showed a weak carbonyl signal (see SI, Figure S6), meaning that the porous structure of the fibers and their hemicellulose content also influence the modification.

The gas-phase reactions were optimized similarly to the BKP_{LE} Kn-reactions on molar ratio and temperature. Initial experiments were performed above the boiling point of itaconic anhydride; however, it was realized that a temperature around the melting point, 66–68 °C, is sufficient for the reaction to occur whilst not discoloring the pulp. Therefore, the reaction was investigated at 50 and 75 °C.

For gas phase reactions, BKP_{LE} Gas, signals for the carbonyl of the ester or carboxylic acid appear around 1710/1725 cm^{-1} and around 1630 cm^{-1} for the C=C (Fig. 7). It is also suspected that the $COO^{-}H^{+}$ overlaps somewhat with the water/carbonyl signal, since a shoulder around 1693 cm^{-1} appears in some of the spectra. There also appears a signal around 1750 cm^{-1}, most likely a product of another isomer. As shown in Fig. 1, the anhydride may react through the C1 or C4 carbon, effectively shifting the placement of the C=C bond, and hence altering the position of the C=O and COOH vibrations.

Discussion

Comparison with prior work

Our observation that kneading promotes substitution within the fiber wall, while gas-phase reactions favor surface modification, is in line with earlier studies. Gas-phase esterification of cellulose has been shown to proceed primarily at accessible surfaces,

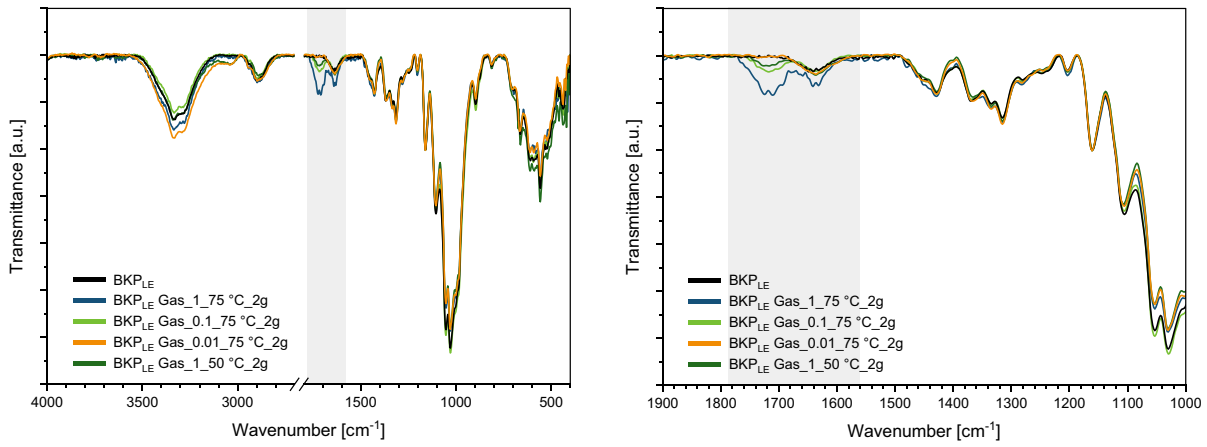

Fig. 7 FTIR spectra of BKP_{LE} Gas reactions with the grey area highlighting the region of interest. Left: Complete spectra of transmittance versus wavenumber [cm^{-1}]. Right: Closeup of the carbonyl region. Molar ratios are expressed as previously explained and the relative signal intensity compared to 1160 cm^{-1}. 50 °C at an equimolar ratio seems to create a similar degree of modification as a lower molar equivalence of 0.1 at 75 °C, indicating that both amount of reagent and temperature are significant for the reaction

with minimal disruption of the bulk structure (David et al. 2019) whereas high-consistency kneading enables reagent penetration into the fiber interior (Duan et al. 2022, Sjölund et. al. 2025). This methodological contrast supports our conclusion that the reaction environment governs the spatial distribution of substitution.

Previous multiscale analyses of cellulose esterification highlight how the choice of method influences both molecular substitution and supramolecular structure (Oberlintner et al. 2022). Our NMR and XRD results—small crystallite size shifts combined with clear changes in surface-sensitive carbons—mirror these findings and emphasize that substitution location, rather than degree alone, dictates functional performance. In terms of chemical reactivity, cyclic anhydrides are well established for cellulose functionalization (Aziz et al. 2022). Our FTIR and titration data confirm the expected introduction of ester and carboxyl functionalities, while also indicating possible isomerization of itaconate under certain conditions. This observation, less commonly addressed in earlier work, highlights the need for deeper mechanistic studies of itaconic reactions with cellulose.

Direct reports on itaconic anhydride are limited, but recent studies demonstrate its ability to form diesters and cross-linked structures (Cheng et al. 2024). These results are consistent with our proposal that itaconic groups provide a versatile platform for further derivatization. Comparisons with maleic anhydride functionalization of fibers show that both reagents introduce carboxylate and alkene functionalities, but the exocyclic double bond of itaconic anhydride offers enhanced opportunities for post-polymerization (Cortes Ruiz et al. 2025). Importantly, other esterification studies confirm that reaction route strongly influences substitution efficiency and performance, supporting our conclusion that "location may overrule quantity" in determining properties such as water retention (Willberg-Keyriläinen and Ropponen 2019). Addressing whether the relatively low degree of substitution (DS values between 0.0139 and 0.1149) has effects on material properties, paper sheets on pristine and modified sheets were made as proof of concept. Clear differences between the papers were found, especially in thickness and roughness of the formed sheet at similar grammages (SI, table S4), with roughness doubling compared to the refence sheet using BKP-itaconate fibers with a DS value of 0.0594. This further strengthens that the modification alters the properties of the pulp.

Broader impact

Itaconic anhydride combines bio-based origin with structural asymmetry and a reactive double bond,

creating a dual functionality: carboxyl groups that modulate fiber–water interactions, and an unsaturation that enables subsequent polymerizations. This duality makes it a promising precursor for designing cellulose fibers with tunable properties, whether for wet-strength enhancement, barrier applications, or composite reinforcement. Its higher reactivity in radical polymerizations compared to maleic anhydride further strengthens its potential as a platform for on-fiber grafting and advanced material development (Kučera et al. 2017).

Equally important is the process control afforded by the two routes studied. Gas-phase esterification provides surface-localized functionality (David et al. 2019), relevant for interfacial adhesion and surface chemistry, whereas kneading enables interior substitution (Duan et al. 2022), influencing swelling, charge distribution, and water management. Such spatial control is directly related to papermaking, where balancing wet-strength and dimensional stability is essential, and to fiber-based composites where interfacial performance governs mechanical behavior.

Limitations and future directions

This study relies on indirect methods—charge titrations, WRV, and FTIR—for assessing substitution location. Although these provide useful trends, complementary depth-resolved techniques (e.g. XPS, ToF–SIMS, AFM-IR) would allow more direct evidence of surface versus interior modification, as demonstrated in related gas-phase esterification studies (David et al. 2019). Likewise, FTIR methods are semi-quantitative. Previous studies conducted on modifications of hemicellulose (Nylander et. Al 2019) managed to extract additional information through multivariate analysis of the FITR spectra, finding patterns and correlations of different modifications, this however was unsuccessful in this study. Combining these with advanced solid-state NMR approaches would strengthen quantitative conclusions (Oberlintner et al. 2022, Höfler et. Al. 2024).

Process variability also remains a limitation. Fiber heterogeneity, moisture content, and kneading efficiency introduce uncertainty, underscoring the value of standardized processing conditions (Duan et al. 2022). The kneading approach can be viewed as a low-shear analogue to extrusion and could readily be adapted to high-consistency industrial mixers or continuous kneaders. Reactive extrusion on cellulose materials is reported in the literature (Guiao et al. 2022). The gas-phase esterification, while less conventional, may be realized using equipment similar to flake or drum dryers operating under controlled vapor atmospheres, suggesting that both reaction routes are technically feasible for scale-up with appropriate process safety measures.

Finally, while we highlight the potential of the itaconate double bond for further polymerization, this work did not yet demonstrate on-fiber grafting. Given the established radical reactivity of itaconic monomers (Kučera et al. 2017), future studies should explore grafting directly from itaconate-modified fibers to translate chemical potential into measurable performance gains.

Conclusion

It was shown that it is possible to modify BKP with ITA through kneading and gas-phase methods, previously not explored. Although the carboxylic acid charge is the same for some of the reactions, their FTIR spectra exposes differences in their chemical bonding, and it seems that itaconic structure isomerize into citraconic or mesaconic structures. Neither the WRV or teabag values showed a clear correlation for water-holding capacity and fiber charge, to some extent contradicting previous findings. It was further shown that different reaction methods (kneading or gas phase) seem to introduce charges at different locations within the fiber structure. This, together with the NMR and XRD studies, concludes that supramolecular changes of the cellulose fibers overrule the charge, that is, that location possibly overrules quantity in terms of material properties, such as water holding capacity. Further, no indications of fiber degradation were observed during or after esterification. The NMR and XRD analyses showed no significant loss of cellulose crystallinity or structural order, and the fibers retained their visual integrity after drying. These observations suggest that the reaction conditions were sufficiently mild to preserve the mechanical characteristics of the cellulose. Finally, this study shows that the esterification of BKP using itaconic anhydride is possible through three different methods, all

generating a functional pulp (BKP-Itaconate), interesting for industrial applications.

Acknowledgement The authors acknowledge funding from the Knut and Alice Wallenberg Foundation (KAW) through the Wallenberg Wood Science Center. Grant number WWSC 3.0: KAW 2021.0313. This work was performed in part at the Chalmers Materials Analysis Laboratory, CMAL.

Author contribution J.F.: Conceptualization, Methodology, Investigation, Data analysis, Visualization, Writing—original draft, Writing—review & editing. Performed all experimental work, conducted and evaluated analyses, prepared figures and compiled data into tables and graphs. P. T. L.: Formal analysis, Writing—review & editing. Contributed to data analysis and interpretation, and reviewed and edited the manuscript. K. M.: Methodology, Writing—review & editing. Proposed complementary experiments, contributed to methodological development, and reviewed the manuscript. G.W.: Conceptualization, Supervision, Methodology, Writing—original draft, Writing—review & editing. Initiated and formulated the project, supervised the work, contributed to manuscript drafting and editing, and participated in data interpretation

Funding Open access funding provided by Chalmers University of Technology. Wallenberg Wood Science Center,WWSC 3.0: KAW 2021.0313.

Data availability Data is available from the authors upon request.

Declarations

Conflicts of interest The authors declare no competing interests.

Consent for publication All authors agreed to the publication in the submitted form.

References

Abson D, Gilbert RD (1980) Observations on water retention values. Tappi 63(9):146

Åhl A, Ruiz-Caldas MX, Nocerino E, Conceição ALC, Nygård K, McDonald S, Viljanen M, Mathew AP, Bergström L (2025) Multimodal structural humidity-response of cellulose nanofibril foams derived from wood and upcycled cotton textiles. Carbohydr Polym 357:123485. https://doi.org/10.1016/j.carbpol.2025.123485

Aziz T, Farid A, Haq F, Kiran M, Ullah A, Zhang K, Li C, Ghazanfar S, Sun H, Ullah R, Ali A, Muzammal M, Shah M, Akhtar N, Selim S, Hagagy N, Samy M, Al Jaouni SK (2022) A review on the modification of cellulose and its applications. Polymers 14(15):3206. https://doi.org/10.3390/polym14153206

Beatson RP (1992) Determination of sulfonate groups and total sulfur. In: Lin SY, Dence CW (eds) Methods in lignin chemistry. Springer, Berlin, Heidelberg, pp 473–484

Börjesson M, Richardson G, Westman G (2015) UV radiation of cellulose fibers and acrylic acid modified cellulose fibers for improved stiffness in paper. BioRes 10(2):3056–3069. https://doi.org/10.15376/biores.10.2.3056-3069

Nippon Paper Group. (2025). Cellulose nanofiber manufacturing technology and application development. From https://www.nipponpapergroup.com/english/research/organize/cnf.html Retrieved: 2025–05–05.

Cheng S, Wang X, Yang R, Wang J, Lu C, Guo K, Zhu N, Hu X (2024) Itaconic anhydride functionalized cyanoethyl cellulose with crosslinked structure enabled improved dielectric properties. Polym Int 73:1022–1029. https://doi.org/10.1002/pi.6680

Cortes Ruiz MF, Martin J, Marcos Celada L, Olsén P, Wågberg L (2025) Strategic functionalization of wood fibers for the circular design of fiber-reinforced hydrogel composites. Cell Rep Phys Sci 6(3):102455. https://doi.org/10.1016/j.xcrp.2025.102455

David G, Gontard N, Guerin D, Heux L, Lecomte J, Molina-Boisseau S, Angellier-Coussy H (2019) Exploring the potential of gas-phase esterification to hydrophobize the surface of micrometric cellulose particles. Eur Polym J 115:138–146. https://doi.org/10.1016/j.eurpolymj.2019.03.002

Duan L, Liu R, Duan Y, Li Z, Li Q (2022) A simultaneous strategy for the preparation of acetylation modified cellulose nanofiber/polypropylene composites. Carbohydr Polym 277:118744. https://doi.org/10.1016/j.carbpol.2021.118744

Ek M, Gellerstedt G, Henriksson G (2009) Ljungberg textbook, volume 3, paper chemistry and technology. KTH, Stockholm, Sweden

Espy HH (1995) The mechanism of wet-strength development in paper: a review

Francolini I, Galantini L, Rea F, Di Cosimo C, Di Cosimo P (2023) Polymeric wet-strength agents in the paper industry: an overview of mechanisms and current challenges. Int J Mol Sci 24(11):9268. https://doi.org/10.3390/ijms24119268

French AD, Santiago Cintrón M (2013) Cellulose polymorphy, crystallite size, and the segal crystallinity Index. Cellulose 20(1):583–588. https://doi.org/10.1007/s10570-012-9833-y

Guiao KS, Gupta A, Tzoganakis C, Mekonnen TH (2022) Reactive extrusion as a sustainable alternative for the

processing and valorization of biomass components. J Clean Prod 355:131840. https://doi.org/10.1016/j.jclepro.2022.131840

Höfler MV, Lins J, Seelinger D, Pachernegg L, Schäfer T, Spirk S, Biesalski M, Gutmann T (2024) DNP enhanced solid-state NMR—a powerful tool to address the surface functionalization of cellulose/paper derived materials. JMRO 21:100163. https://doi.org/10.1016/j.jmro.2024.100163

Hult E-L, Larsson PT, Iversen T (2002) A comparative CP/MAS 13C-NMR study of the supermolecular structure of polysaccharides in Sulphite and Kraft pulps. Holzforschung 56(2):179–184. https://doi.org/10.1023/A:1009236932134

Isogai A, Saito T, Fukuzumi H (2011) TEMPO-oxidized cellulose nanofibers. Nanoscale 3(1):71–85. https://doi.org/10.1039/C0NR00583E

Jayme G (1958) Properties of wood celluloses. II. Determination and significance of water-retention value. Tappi J 41(11):180A

Kučera F, Petruš J, Matláková J, Jančář J (2017) Itaconic anhydride homopolymerization during radical grafting of poly(lactic acid) in melt. React Funct Polym 116:49–56. https://doi.org/10.1016/j.reactfunctpolym.2017.05.004

Lindgren J, Öhman LO, Gunnars S, Wågberg L (2002) Charge determinations of cellulose fibres of different origin—comparison between different methods. NPPRJ 17(1):89–96. https://doi.org/10.3183/npprj-2002-17-01-p089-096

Lindström T, Wågberg L and Larsson T (2005/2018) Review: On the nature of joint strength in paper—A review of dry and wet strength resins used in paper manufacturing. Advances in Paper Science and Technology. Trans. of the XIIIth Fund. Res. Symp. Cambridge, 2005, (S.J. I'Anson, ed.), pp 457–562, FRC, Manchester, 2018

Malmgren K and Nordqvist T (2023). Production of modified pulp. U. S. Patent 11,739,477 B2, SCA Forest Products AB (Sundsvall).

Nylander F, Svensson O, Josefson M, Larsson A, Westman G (2019) New features of arabinoxylan ethers revealed by using multivariate analysis. Carbohydr Polym 204:255–261. https://doi.org/10.1016/j.carbpol.2018.09.062

Oberlintner A, Huš M, Likozar B, Novak U (2022) Multiscale study of functional acetylation of cellulose nanomaterials by design: ab initio mechanisms and chemical reaction microkinetics. ACS Sustain Chem Eng 10(47):15480–15489. https://doi.org/10.1021/acssuschemeng.2c04686

Onur A, Ng A, Garnier G, Batchelor W (2019) The use of cellulose nanofibres to reduce the wet strength polymer quantity for development of cleaner filters. J Clean Prod 215:226–231. https://doi.org/10.1016/j.jclepro.2019.01.017

Patterson AL (1939) The Scherrer Formula for X-Ray particle size determination. Phys Rev 56(10):978–982. https://doi.org/10.1103/PhysRev.56.978

Roberts JC (1996) The Chemistry of Paper. UK, The Royal Society of Chemistry, Cambridge

Salmén L, Stevanic JS (2018) Effect of drying conditions on cellulose microfibril aggregation and "hornification." Cellulose 25(11):6333–6344. https://doi.org/10.1007/s10570-018-2039-1

Scherrer P. (1918). Bestimmung der Größe und der inneren Struktur von Kolloidteilchen mittels Röntgenstrahlen. Nachrichten von der Gesellschaft der Wissenschaften zu Göttingen, Mathematisch-Physikalische Klasse 1918.

Shokri A, Abedin A, Fattahi A, Kass SR (2012) Effect of hydrogen bonds on pKa values: Importance of networking. J Am Chem Soc 134(25):10646–10650. https://doi.org/10.1021/ja3037349

Sjölund J, Westman G, Wågberg L, Larsson PA (2025) High-consistency modification of cellulose fibers: resource-efficient introduction of cationic charges, and their effect on fiber and nanofibril properties. Carbohydr Polym 352:123254. https://doi.org/10.1016/j.carbpol.2025.123254

Stenstad P, Andresen M, Tanem BS, Stenius P (2008) Chemical surface modifications of microfibrillated cellulose. Cellulose 15(1):35–45. https://doi.org/10.1007/s10570-007-9143-y

Tarrés Q, Oliver-Ortega H, Alcalà M, Merayo N, Balea A, Blanco Á, Mutjé P, Delgado-Aguilar M (2018) Combined effect of sodium carboxymethyl cellulose, cellulose nanofibers and drainage aids in recycled paper production process. Carbohydr Polym 183:201–206. https://doi.org/10.1016/j.carbpol.2017.12.027

Terrett OM, Lyczakowski JJ, Yu L et al (2019) Molecular architecture of softwood revealed by solid-state NMR. Nat Commun 10:4978. https://doi.org/10.1038/s41467-019-12979-9

Weise U, Maloney T, Paulapuro H (1996) Quantification of water in different states of interaction with wood pulp fibres. Cellulose 3:189–202. https://doi.org/10.1007/BF02228801

Wickholm K, Larsson PT, Iversen T (1998) Assignment of non-crystalline forms in cellulose I by CP/MAS 13C NMR spectroscopy. Carbohydr Res 312(3):123–129. https://doi.org/10.1016/S0008-6215(98)00236-5

Willberg-Keyriläinen P, Ropponen J (2019) Evaluation of esterification routes for long chain cellulose esters. Heliyon 5(11):e02898. https://doi.org/10.1016/j.heliyon.2019.e02898

Winter L, Wågberg L, Ödberg L, Lindström T (1986) Polyelectrolytes adsorbed on the surface of cellulosic materials. J Colloid Interface Sci 111(2):537–543. https://doi.org/10.1016/0021-9797(86)90057-3

Wongvitvichot W, Pithakratanayothin S, Wongkasemjit S, Chaisuwan T (2021) Fast and practical synthesis of carboxymethyl cellulose from office paper waste by ultrasonic-assisted technique at ambient temperature. Polym Degrad Stabil 184:109473. https://doi.org/10.1016/j.polymdegradstab.2020.109473

Zhang H, Tsenter E, Bicho P, Doherty AES, Riehle R, Moran-Mirabal J, Pelton RH (2021) Carboxylated bleached kraft pulp from maleic anhydride copolymers. Nat Prod Res J 36(4):608–617. https://doi.org/10.1515/npprj-2021-0005